

Graphenated ceramic nanofibers for highly sensitive simultaneous detection of dopamine, uric acid and ascorbic acid

Masoud Taleb¹, Irina Hussainova^{1,2,3*}, Roman Ivanov¹, Iwona Jasiuk³

¹Tallinn University of Technology, Department of Materials Engineering, Ehitajate 5, Tallinn, Estonia

²ITMO University, Kronverksky 49, St. Petersburg, Russian Federation

³University of Illinois at Urbana-Champaign, Department of Mechanical Science and Engineering, Urbana, IL 61801, USA

*Corresponding author: Tel: (+372) 6203371; E-mail: irina.hussainova@ttu.ee

Received: 18 December 2016, Revised: 05 February 2017 and Accepted: 07 April 2017

DOI: 10.5185/amlett.2017.1557

www.vbripress.com/aml

Abstract

The present study reports the simultaneous determination of ascorbic acid (AA), dopamine (DA) and uric acid (UA) in 0.1 M phosphate buffer solution (pH = 7.0) using a novel electrode material prepared from oxide ceramic nanofibers by applying a single step chemical vapor deposition method. Electron-transfer kinetics at the electrode/solution interface was studied by standard redox reaction of 5 mM $\text{Fe}(\text{CN})_6^{3-/4-}$ in 1 M KCl. Electrochemical and sensing measurements such as cyclic voltammetry and differential pulse voltammetry were performed to detect DA and UA in the presence of AA. The developed electrode was shown to separate the overlapping voltammetric responses of three analytes into the individual voltammetric peaks, totally eliminate the interference from AA, and distinguish DA from UA. Linear relationship was observed between current intensities and concentrations of all three compounds, and the limits of detection (LOD) were reached 0.57 μM , 0.77 μM and 0.84 μM for DA, UA and AA, respectively. The electrode of graphenated nanofibers displayed a very good reproducibility and stability, and was successfully tested for detection of DA, UA and AA in real urine samples. Copyright © 2017 VBRI Press.

Keywords: Graphene, ascorbic acid, dopamine, uric acid, voltammetry.

Introduction

Dopamine (DA), uric acid (UA) and ascorbic acid (AA) are compounds of a great biomedical interest, which play a fundamental role in human metabolism [1]. Dopamine is one of the most important neurotransmitters that controls the function of the central nervous system, renal and the balance of hormones in a human body. Abnormal level of DA can cause several neurological diseases, including Schizophrenia, Parkinson's disease, HIV, and Alzheimer's diseases [2]. UA is another important biomolecule in a human body, which is the primary product of purine metabolism. Its abnormal level of concentration points to several possible diseases such as gout, hyperuricemia, and Lesch-Nyhan syndrome [3]. On the other hand, AA is a vital component known for its antioxidant peculiarity and its role in treatment of the common cold, mental illness, and infertility [4]. Since AA, DA, and UA are electroactive compounds and coexist in physiological fluids, development of a technique for effective, selective and simultaneous detection has recently received considerable interest. Electrochemical techniques have been widely applied due to fast detection, simplicity, reproducibility, and cost-effectiveness. However, the electrochemical oxidation

potentials of AA, DA, and UA are very close and obtained response can easily be affected by the presence of other biomolecules. In order to overcome this problem, a wide variety of materials have been tested in order to improve the electrocatalytic performance of the electrode surface to separate their oxidation potentials [5, 6]. Among studied materials, carbon nanostructures and, especially, graphene have been utilized for surface modification of the electrode due to their unique structures, outstanding charge-transfer properties and good chemical stability [7, 8]. The advanced analytical approaches require high sensitivity and selectivity combined with simplicity of sample manufacturing and its modification added by good stability and signal enhancement as compared to bare electrodes. A linear working concentration range, clear separation between oxidation peak potentials and low limit of detection are essential criteria to be met for development of a novel electrode material. As electrochemical sensors, many advanced electrode interfaces were constructed through modification of electrode surface with graphene or its composites, which can effectively decrease the overpotential and enhance the current response. It is widely documented that any surface modifications can

play a catalytic role and very small changes in surface characteristics can determine the sensitivity of measurement in electroanalytical applications. Therefore, the reliable and precisely monitored procedure for fabrication of modified electrodes is of particular importance for clinical applications.

In this work, by combining the unique electronic properties of graphene with a large surface area of self-aligned ceramic nanofibers, a highly sensitive sensor was developed for simultaneous determination of DA, UA, and AA. The nanofibers covered by highly foliated multi-layer graphene were produced with the help of a simple and well – controllable single-step chemical vapor deposition (CVD) process and electrochemically studied using cyclic voltammetry (CV) and differential pulse voltammetry (DPV) techniques. It is believed that graphitic edge planes/defects are essentially responsible for the fast electron-transfer (ET) kinetics and excellent sensing and biosensing performance [9]. At the present study, the CVD process was adjusted to get a high density of graphenic foliates to ensure fast electron-transfer kinetics and an excellent electrocatalytic activity for simultaneous determination of dopamine (DA), ascorbic acid (AA) and uric acid (UA). Furthermore, the developed electrode was successfully evaluated in human urine samples presenting good sensitivity and selectivity.

Experimental

Materials and reagents

All reagents and materials were of analytical grade and used as received. All the solutions were prepared using a Millipore water (18.2 M Ω .cm, Millipore water Ltd., USA). The 0.1 M phosphate buffer solution with pH 7.0 that is close to a human blood pH value was prepared by mixing 0.1 M K₂HPO₄ and 0.1 M KH₂PO₄ with the 0.1 M HCl as the supporting electrolyte. Potassium ferrocyanide, AA, DA and UA were purchased from Organics. The stock solutions of AA, DA and UA were freshly prepared in phosphate buffer solution at room temperature (22 ± 1 °C).

A network of the well-aligned alumina nanofibers was developed by a controlled liquid phase oxidation of aluminium melt as described in [10]. The graphenated Al₂O₃ fibers (a single fiber diameter was of 7±2 nm) were prepared by deposition of highly foliated graphene layers onto the surface of self-aligned oxide ceramic fibers through a CVD process under methane (CH₄) gas flow of 200 cm³ min⁻¹ and at temperature of 1000 °C as described elsewhere [11-13]. Schematic representation of the fabrication process is shown in Fig. 1. The particularly attractive fact is that the hybrid graphene/alumina nanofibers were produced without the use of catalysts, although their growth mechanism is still not completely understood.

The weight gain after the treatment was 700 %. Thus, the material to be used for preparation of the electrode was named ANF-C700 indicating weight gain of carbon on alumina nanofibers (ANF).

The array of the graphenated fibers was crushed by mortar and additionally powdered using MLW KM1 ball milling machine and Hielscher UP200S ultrasonic processor (power 100 watts) in presence or absence of tungsten carbide (WC, particles size 370±25 μ m) powder based on optimized conditions shown in Table 1. The WC particles were used in order to elucidate a role of hard particles in a wet-milling and micro-grinding of the specimens as discussed in [14].

Table 1. Optimization of experiments by varying powder preparations techniques.

Sample	Mortar	Ball milling	Presence of WC	Ultrasound treatment
Sample 1	√	-	-	10 min in water
Sample 2	√	-	√	10 min in water
Sample 3	√	30 min	√	10 min in water
Sample 4	√	30 min	-	10 min in water
Sample 5	√	180 min	-	30 min in isopropanol

The obtained powders were suspended in an optimum amount of isopropanol and Nafion[®] dispersion solution as described in [15], agitated for 30 min in an ultrasonic bath, drop casted on a polished glassy carbon disk electrode (GCE) and dried in room temperature.

Characterization

Electrochemical measurements, i.e. cyclic voltammetry and differential pulse voltammetry, were performed in a potentiostat/galvanostat Autolab PGSTAT30 in a standard three - electrode electrochemical cell. A GCE modified with ANF-C700, a Pt wire and a saturated calomel electrode (SCE) were used as the working, counter and reference electrodes, respectively.

The morphology and physical properties of the developed material were studied by scanning electron microscopy (SEM, Zeiss HR FESEM Ultra 55), high resolution transmission microscopy (HR-TEM, JEOL 2100F), and X-ray photoelectron spectroscopy (XPS, Omicron Multiprobe XPS system). Materials characterization performed by X-ray diffraction (XRD, Bruker) and Raman spectroscopy (Horiba's LabRam HR800) is detailed in [16].

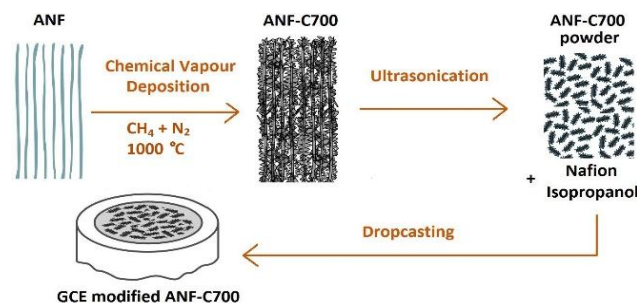


Fig. 1. Schematic representation of the fabrication of GCE modified with ANF-C700

Results and discussion

Characterization of ANF-C700

The Raman spectra [14], SEM and TEM examination confirmed presence of several layers of highly defected graphene with graphene sheet foliates grown on sidewalls of the outer layers of graphene wraps around the longitudinal axis of the nanofiber. Mass gain of 700 % corresponds to 5 – 15 layers of graphene-like layers with lots of admixture of the graphitic flakes developing the hybrid nanostructure of closed shell of graphene multi-layers and nano-foliates with a high density of open edges. The advantages of exploitation of such kind of structure are relatively large surface area, high electrical conductivity, simple and controllable single-step method of preparation, and good stability of the structure. The graphene nano-foliates are randomly entangled and cross-linked on the surface of graphene. Representative images of the graphene-decorated fibers are given in (Fig. 2a, b and c). Fig. 1b reveals that the majority of graphene foliates have a preferentially perpendicular orientation with respect to the fiber surface.

Density of the foliates was calculated to be 50 ± 10 per micron length of the fiber. An average fiber diameter after treatment was 45 ± 10 nm providing a specific surface area of $120 \text{ m}^2 \text{ g}^{-1}$ (BET).

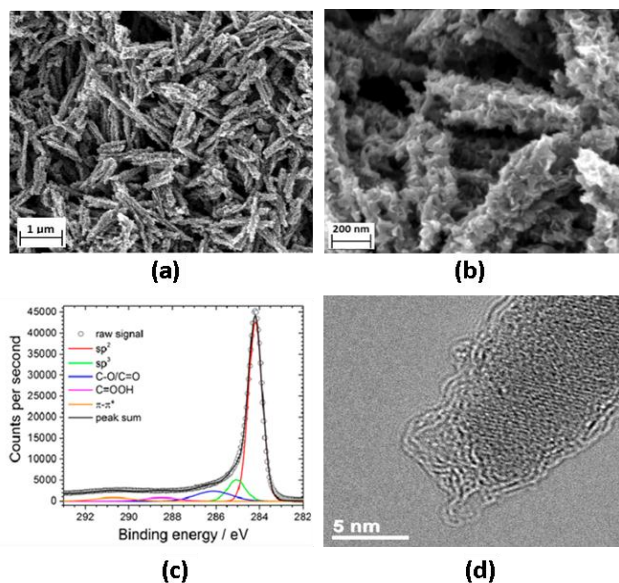


Fig. 2. (a), (b) SEM images of ANF-C700 sample 4; (c) XPS spectrum of ANF-C700; (d) TEM micrograph of a single fiber covered by foliated graphene.

XPS analysis exhibited a low content of oxygen, thus indicating that the growth process leads to the deposition of a film with high carbon purity [16], (Fig. 2d). The sp^2 -associated peak at 284.3 eV attributed to the highest contribution of trigonally bonded carbon. After the subtraction of a Shirley background followed by fit using a mixture function of Lorentzian and Gaussian, the C 1s peak can be mainly deconvoluted into five sub-peaks, which have been assigned to C-C (sp^2), so-called “defect peak” with 0.5 eV energy shift, C-O and C=O bonds,

respectively. This demonstrates that the foliated carbon nanostructures consist of metal-free graphitic materials with some oxygen adsorbates due to physical adsorption of oxygen or vapor mainly on the edge defects at room temperature after exposure of the sample to air.

Fig. 3a schematically shows the structure of a single fiber used for the simultaneous detection of AA, DA, and UA.

Electrochemical behavior of sample

For optimization of the experiments, five distinct samples prepared from the ANF-C700 powders and the bare GC electrode, indicated in Table 1, were studied for their electrocatalytic activity in 1 M KCl + 5 mM $\text{K}_3\text{Fe}(\text{CN})_6$ system.

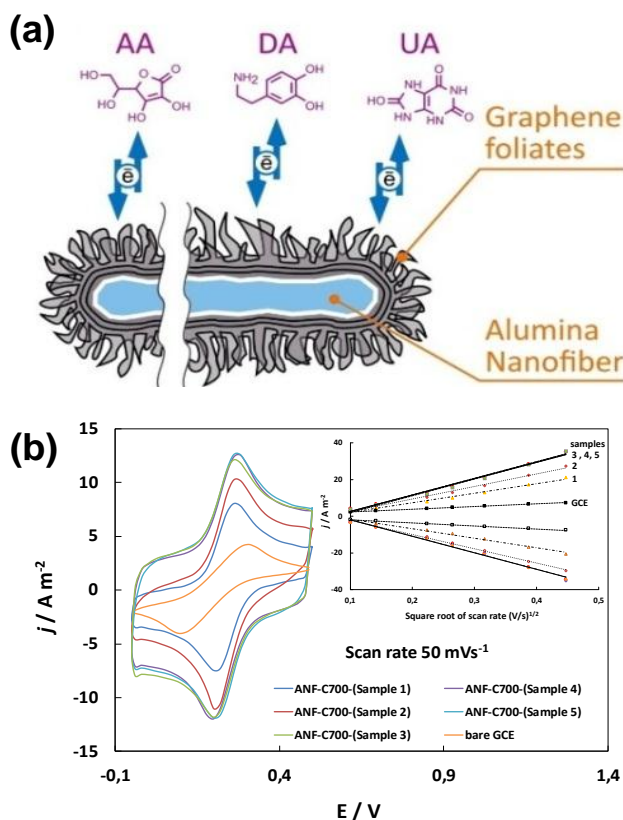


Fig.3. (a) Schematic representation of the structure of the single ANF-C700 fiber; (b) CV responses of comparative voltammograms of ANF-C700 electrodes. Inset - the linear relation of the anodic and cathodic peak currents against the square root of potential scan rates in the range of 10 to 200 mV s^{-1} .

Fig. 3 displays the voltammograms of differently prepared ANF-C700 modified electrodes at a scan rate of 50 mV s^{-1} . The bare GCE exhibits a wide peak with and a peak to peak separation of 210 mV representing a quasi-reversible reaction. In contrast, the ANF-C700 electrodes present significantly higher peak currents with a redox potential difference (ΔE_p) ranging 60–65 mV, indicating that the process under consideration is approximately reversible and reaction is diffusion controlled, similar to that observed, for example, for Ag nanoparticles [17].

According to the obtained results, the sample 4 (see Table 1) prepared by 30 min milling in water without WC, was chosen for further consideration due to its well-pronounced oxidation peak.

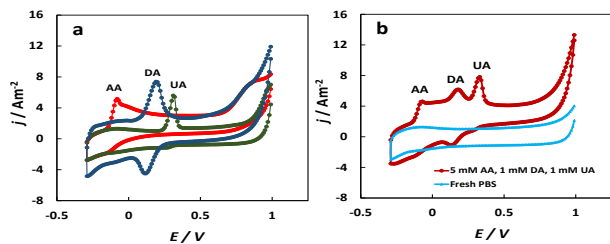


Fig. 4. CV responses of (a) individual sensing of 5 mM AA, 1 mM DA, and 1 mM UA; (b) ternary mixture of 5 mM AA, 1 mM DA, and 1 mM UA in 0.1 M phosphate buffer solution (pH 7.0) on ANF-C700 at 10 mV s^{-1} .

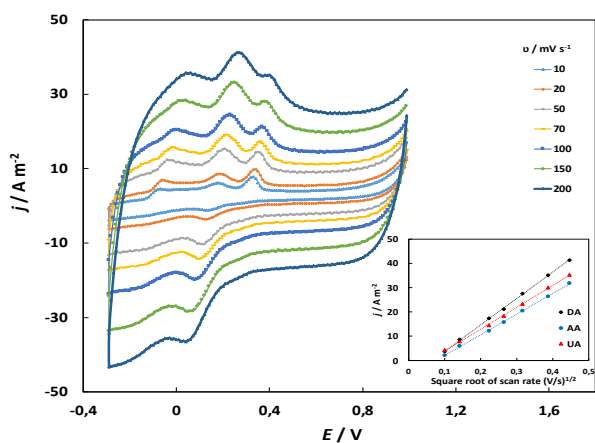


Fig. 5. Effect of scan rate on sensing mixture of 5 mM AA, 1 mM DA, and 1 mM UA in 0.1 M phosphate buffer solution with pH 7.0 (Inset - plots of peak current versus square root of the scan rate at 10, 20, 40, 70, 100, 150, 200 mV s^{-1})

Cyclic voltammetric detection of DA, UA and AA on the ANF-C700

Cyclic voltammetry technique was used to investigate the electrocatalytic activity of the developed electrode by adding AA, DA and UA ranging from -0.3 to 1 V (vs. SCE) in 0.1 M pH 7.0 phosphate buffer solution (Fig. 4a, b). A large peak-potential separation was obtained at pH 7.0 . The voltammetric responses of these biomolecules show the well-defined and resolved oxidation peaks at -60 mV , 210 mV and 320 mV for AA, DA and UA, respectively. The reduction peak for AA is resolved; however, for DA a clearly separated peak is found at 120 mV . In case of UA, a weak reduction peak is observed at 280 mV . In order to demonstrate the selective and sensitive behavior of the electrode, a mixture of AA, DA and UA was tested in phosphate buffer solution by CV. The cyclic voltammograms of ternary mixture containing 5 mM AA, 1 mM DA, and 1 mM UA, shown in (Fig. 4b), clearly present three well-recognized anodic peaks corresponding to AA, DA and UA at -40 mV , 200 mV and 340 mV , respectively. This separation indicates that the interference between AA, DA and UA oxidation potential is eliminated by utilizing ANF-C700. The

anodic peak interval potentials were 240 mV , 140 mV and 380 mV for AA-DA, DA-UA and AA-UA, respectively. Besides, a strong cathodic peak of DA was observed at 150 mV . The obtained results show that the synthesized ANF-C700 material exhibits an excellent selective electrocatalytic behavior for the simultaneous electro-oxidation of three bio-analytes being under consideration.

Fig. 5 displays the cyclic voltammograms of the developed sensor in presence of 5 mM AA, 1 mM DA, and 1 mM UA. The oxidation peak currents increase consistently with increase in a scan rate from 10 up to 200 mV s^{-1} . A linear relationship between the anodic peak current and square root of scan rate was observed for oxidation of AA, DA or UA.

The oxidation peaks current increases with the scan rate, and the oxidation peak potential is shifted positively, while the reduction peak potential shifts negatively.

The CV results show that ANF-C700 is able to determine not only AA, DA, and UA individually, but also separate them in the mixture of these biomolecules, demonstrating the negligible interfering effect from interactions among AA, DA and UA.

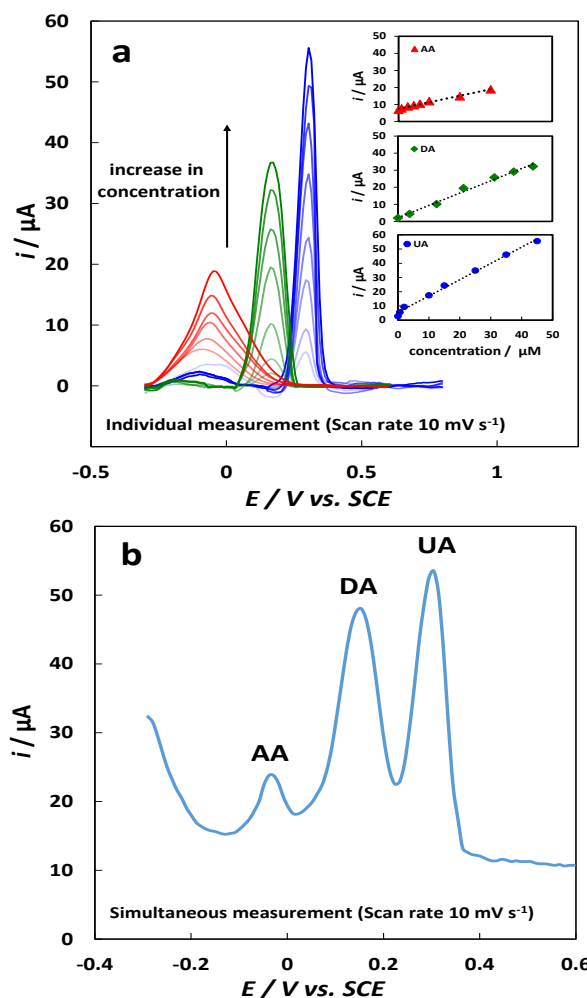


Fig. 6. DPV response at ANF-C700 electrode (a) individual sensing of AA, DA, and UA concentrations from 5 nM to 45 μM ; and (b) mixture of 50 μM AA, 60 μM DA, 50 μM UA in phosphate buffer solution (pH 7.0) at a scan rate of 10 mV s^{-1} .

Table 2. Performance of different electrodes for simultaneous determination of AA, DA and UA.

Electrode	Linear range (μM)			LoD (μM)			Reference s
	AA	DA	UA	AA	DA	UA	
Helical CNTs	7.5–180	2.5–105	6.7–65	0.92	0.8	1.5	[19]
Tryptophan-graphene	0.2–12.9	0.5–110	10–1000	10.09	0.29	1.24	[20]
SWCNH	30–400	0.2–3.8	0.06–10	5	0.06	0.02	[21]
N-doped graphene	5–1300	0.5–170	0.1–20	2.2	0.25	0.045	[22]
ANF-C700	0.005–30	0.005–45	0.005–45	0.84	0.57	0.77	This work

Determination of DA, UA and AA on the ANF-C700 by differential pulse voltammetry

To study the sensitivity and defining linear ranges, the differential pulse voltammetry (DPV) data of the developed electrode were collected in 0.1 M pH 7.0 phosphate buffer solution in the presence of AA, DA, and UA, as shown in (Fig. 6a, b). The oxidation peaks of AA, DA and UA are clearly separated from each other confirming the results obtained by CV. The oxidation peak currents increase linearly with an increase in concentrations of bio-analytes providing the steady peak potentials at -28 mV, 183 mV and 314 mV for AA, DA and UA, respectively. The linear ranges of AA, DA and UA are found as $0.005\text{--}30$ μM , $0.005\text{--}45$ μM and $0.005\text{--}45$ μM and the detection limits ($S/N = 3$) are 0.84 μM and 0.57 μM , and 0.77 μM . Corresponding linear regression equations can be expressed as follows: I_p AA (μA) = $0.3814x + 7.5176$ (μM) ($R = 0.9905$); I_p DA (μA) = $0.8798x + 2.4099$ (μM) ($R = 0.9919$); and I_p UA (μA) = $2.638x + 3.6626$ (μM) ($R=0.9986$). The DPV results for the mixture of AA, DA and UA show that the ANF-C700 is able to selectively detect each of the interfering compounds (Fig. 6a, b). Table 2 presents a comparison between current study and some other works indicating that ANF-C700 has comparable or even better analytical performance to be applied in sensor applications.

Real samples analysis

In order to study the selectivity of the ANF-C700 electrode in the real samples, a human urine was selected as a biological object. Three urine samples were tested for detection of their AA, DA, and UA levels. The test samples were diluted 50-fold before use with pH 7.0 phosphate buffer solution to prevent the matrix effect of the authentic samples. The DPV technique was applied to ascertain the results before and after the samples were spiked with 30 μM AA, 20 μM DA and 10 μM UA. Recovery rates of the samples were found to be between 95.5% and 106% , indicating that ANF-C700 material can be effectively utilized for the simultaneous determination of AA, DA, and UA in the real samples analysis. Anti-interference ability of the fabricated sensor, studied in previous work [18], showed very clear amperometric signal of AA, DA and UA; while addition of common interfering compounds such as ammonium chloride, FeCl_3 , MgCl_2 , KCl , citric acid, Na_2SO_4 , NaCl , Urea and H_2O_2 did not affect the response (signal change $<3\%$).

Conclusions

In summary, the ceramic nanofibers were coated by highly foliated graphene deposited by a simple single – step CVD process, and employed to develop a sensor for simultaneous selection of several important bio-molecules such as AA, DA, and UA. The electrode of GCE modified with ANF-C700 was tested for its electrochemical and showed not only high sensitivity and selectivity toward individual detection of AA, DA and UA, but also successfully resolved their overlapped oxidation peaks into three well-defined peaks.

High selectivity and good antifouling ability of ANF-C700 electrode was proved by simultaneous determination of AA, DA and UA in a ternary mixture of these bio-analytes.

The excellent analytical performance and successful application of this electrode on human urine sample suggests ANF-C700 as a promising candidate applicable for highly sensitive and selective electrochemical sensors.

Acknowledgements

This research was supported by the Estonian Research Council under the personal grant PUT1063 (I. Hussainova). The authors also acknowledge Estonian Ministry of Higher Education and Research under the Project IUT19-29 as well as Baltic-American Freedom Foundation under a research grant to I. Hussainova. The TEM examination was carried out in the Frederick Seitz Materials Research Laboratory Central Facilities, University of Illinois at Urbana-Champaign, USA.

References

- Argüello, J., V.L. Leidens, H.A. Magosso, R.R. Ramos, et al., *Electrochim. Acta.*, **2008**, *54*, 560.
DOI: [10.1016/j.electacta.2008.07.021](https://doi.org/10.1016/j.electacta.2008.07.021)
- Mo, J.-W. and B. Ogorevc, *Anal. Chem.*, **2001**, *73*, 1196.
DOI: [10.1021/ac0010882](https://doi.org/10.1021/ac0010882)
- Zou, H.L., B.L. Li, H.Q. Luo, and N.B. Li, *Anal. Biochem. B: Chemical*, **2015**, *207*, 535.
DOI: [10.1016/j.snb.2014.10.121](https://doi.org/10.1016/j.snb.2014.10.121)
- Atta, N.F., M.F. El-Kady, and A. Galal, *Anal. Biochem.*, **2010**, *400*, 78.
DOI: [10.1016/j.ab.2010.01.001](https://doi.org/10.1016/j.ab.2010.01.001)
- Wang, H., P. Jiang, X. Bo, and L. Guo, *Electrochim. Acta.*, **2012**, *65*, 115.
DOI: [10.1016/j.electacta.2012.01.027](https://doi.org/10.1016/j.electacta.2012.01.027)
- Zhang, W., R. Yuan, Y.-Q. Chai, Y. Zhang, et al., *Sensors and Actuators B: Chemical*, **2012**, *166*, 601.
DOI: [10.1016/j.snb.2012.03.018](https://doi.org/10.1016/j.snb.2012.03.018)
- McCreery, R.L., *Chemical Reviews*, **2008**, *108*, 2646.
DOI: [10.1021/cr068076m](https://doi.org/10.1021/cr068076m)

8. Xiao, C., X. Chu, Y. Yang, X. Li, et al., *Biosens. Bioelectron.*, **2011**, 26, 2934.
DOI: [10.1016/j.bios.2010.11.041](https://doi.org/10.1016/j.bios.2010.11.041)
9. Shang, N.G., P. Papakonstantinou, M. McMullan, M. Chu, et al., *Adv. Funct. Mater.*, **2008**, 18, 3506.
DOI: [10.1002/adfm.200800951](https://doi.org/10.1002/adfm.200800951)
10. Aghayan, M., I. Hussainova, M. Gasik, M. Kutuzov, et al., *Thermochim. Acta.*, **2013**, 574, 140.
DOI: [10.1016/j.tca.2013.10.010](https://doi.org/10.1016/j.tca.2013.10.010)
11. Ivanov, R., V. Mikli, J. Kübarsepp, and I. Hussainova, *Key Engineering Materials*, **2016**, 674, 77.
DOI: [10.4028/www.scientific.net/KEM.674.77](https://doi.org/10.4028/www.scientific.net/KEM.674.77)
12. Ivanov, R., I. Hussainova, M. Aghayan, M. Drozdova, et al., *J. Eur. Ceram. Soc.*, **2015**, 35, 4017.
DOI: [10.1016/j.jeurceramsoc.2015.06.011](https://doi.org/10.1016/j.jeurceramsoc.2015.06.011)
13. Hussainova, I., R. Ivanov, S.N. Stamatina, I.V. Anoshkin, et al., *Carbon*, **2015**, 88, 157.
DOI: [10.1016/j.carbon.2015.03.004](https://doi.org/10.1016/j.carbon.2015.03.004)
14. Bang, J.H. and K.S. Suslick, *Adv. Mater.*, **2010**, 22, 1039.
DOI: [10.1002/adma.200904093](https://doi.org/10.1002/adma.200904093)
15. Taleb, M., J. Nerut, T. Tooming, T. Thomberg, et al., *J. Electrochem. Soc.*, **2016**, 163, F1251.
DOI: [10.1149/2.1051610jes](https://doi.org/10.1149/2.1051610jes)
16. Stamatina, S.N., I. Hussainova, R. Ivanov, and P.E. Colavita, *ACS Catalysis*, **2016**, 6, 5215.
DOI: [10.1021/acscatal.6b00945](https://doi.org/10.1021/acscatal.6b00945)
17. Lin, Y., L. Li, L. Hu, K. Liu, et al., *Sensors and Actuators B: Chemical*, **2014**, 202, 527.
DOI: [10.1016/j.snb.2014.05.113](https://doi.org/10.1016/j.snb.2014.05.113)
18. Taleb, M.; Ivanov, R.; Bereznev, S.; Kazemi, S. H.; Hussainova, I., *Microchimica Acta*, **2017**, 184, 897.
DOI: [10.1007/s00604-017-2085-7](https://doi.org/10.1007/s00604-017-2085-7)
19. Cui, R., X. Wang, G. Zhang, and C. Wang, *Sensors and Actuators B: Chemical*, **2012**, 161, 1139.
DOI: [10.1016/j.snb.2011.11.040](https://doi.org/10.1016/j.snb.2011.11.040)
20. Lian, Q., Z. He, Q. He, A. Luo, et al., *Anal. Chim. Acta.*, **2014**, 823, 32.
DOI: [10.1016/j.aca.2014.03.032](https://doi.org/10.1016/j.aca.2014.03.032)
21. Zhu, S., H. Li, W. Niu, and G. Xu, *Biosens. Bioelectron.*, **2009**, 25, 940.
DOI: [10.1016/j.bios.2009.08.022](https://doi.org/10.1016/j.bios.2009.08.022)
22. Sheng, Z.-H., X.-Q. Zheng, J.-Y. Xu, W.-J. Bao, et al., *Biosens. Bioelectron.*, **2012**, 34, 125.
DOI: [10.1016/j.bios.2012.01.030](https://doi.org/10.1016/j.bios.2012.01.030)